Food Chemistry: X 21 (2024) 101204

Contents lists available at ScienceDirect

Food Chemistry: X

journal homepage: www.sciencedirect.com/journal/food-chemistry-x

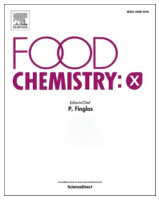

Interaction of the extracellular protease from *Staphylococcus xylosus* with meat proteins elucidated via spectroscopic and molecular docking

Hui Wang [a,b], Siqi Zhao [b], Xiufang Xia [b], Jun Liu [c], Fangda Sun [b,*], Baohua Kong [b,*]

[a] School of Food Science, Henan Institute of Science and Technology, Xinxiang 453003, China
[b] College of Food Science, Northeast Agricultural University, Harbin, Heilongjiang 150030, China
[c] Shandong Yuwang Ecological Food Industry CO., Ltd., Yucheng 251200, China

ARTICLE INFO

Keywords:
Meat protein
Staphylococcus xylosus protease
Conformation
Flavor
Molecular docking

ABSTRACT

This study aimed to assess the effect of an external protease secreted by *Staphylococcus* (*S.*) *xylosus* on the hydrolysis and flavor properties of meat protein. The results indicated that the protease significantly increased the solubility of myofibrillar proteins (MPs) and sarcoplasmic proteins (SPs) in water ($P < 0.05$), and altered their surface hydrophobicity and secondary structure. The results of micromorphological and free amino acids analyses suggested that the protease degraded the large and insoluble meat protein aggregates into small molecular proteins with uniform distribution and amino acids, especially glycine, glutamic acid, leucine, and cysteine. Moreover, the protease-catalyzed hydrolysis promoted the formation of some volatile compounds in the MPs and SPs. Additionally, molecular docking analysis suggested that hydrogen bond and hydrophobic interaction promoted the formation of a *S. xylosus* protease/meat protein complex. These results provided a basis for the future application of *S. xylosus* protease in meat products.

1. Introduction

Important components of meats myofibrillar proteins (MPs; salt-soluble) and sarcoplasmic proteins (SPs; water-soluble) account for 50 % and 30 %–35 % of the total meat proteins content, respectively. They contain all of the essential amino acids that contribute to the nutritional value of meat products made from them (Wang, Xu, Kong, Liu, Xia, & Sun, 2022). Normally, consumer acceptance of meat products is determined by flavor, especially fermented ones. Proteolysis has been proven to be one of the major processes involved in ripening and flavor development in fermented meat products (Feng, Qiao, Zou, Huang, Kang, & Zhou, 2014; Zhang et al., 2017). Although protein itself has no flavor, the peptides and free amino acids (FAAs) produced by a series of degradation processes are precursors of flavor compounds or are the actual compounds that contribute to both the taste and aroma of a product (Barros et al., 2019; Chen, Xu, & Zhou, 2016). Cathepsins, trypsin-like peptidases and microbial proteases are the main endogenous and exogenous enzymes responsible for the proteolysis of meat (Berardo et al., 2017). Although endogenous enzymes are primarily responsible for the proteolysis throughout the fermentation period, while some endogenous enzymes may be inhibited by fermentation conditions in the later stage of fermentation, reducing the efficiency of proteolysis by endogenous enzymes. Therefore, microbial proteases play a significant role in the proteolysis in the later stage of fermentation (Cachaldora, Fonseca, Franco, & Carballo, 2013). The outcomes from several studies suggest that exogenous proteases produced by microorganisms can degrade meat protein into precursors of flavor compounds in the later stages of fermentation, thereby promoting the formation of the final product flavor (Chen, Liu, Sun, Kong, & Xiong, 2015b).

Coagulase-negative staphylococci (CNS) such as *Staphylococcus* (*S.*) *xylosus* and *S. carnosus* are the most common beneficial bacteria present in meat products (Hu, Chen, Wen, Wang, Qin, & Kong, 2019). They mainly improve the color and flavor of meat products by secreting nitrate reductases, proteases, and lipases. Wang, Zhao, Su, and Jin (2019) reported that dry fermented mutton inoculated with *S. carnosus* attained a relatively high degree of proteolysis, which is possible due to a protease secreted by the bacterium promoting proteolysis. Xiao, Liu, Chen, Xie, and Li (2020) reported that sausages inoculated with *S. xylosus* exhibited a high total FAA content and an enhanced flavor, which may be because the bacterium secretes a protease that promotes the conversion of meat proteins into amino acids, thereby improving the flavor of the sausages. In a previous study, we showed that *S. xylosus* secretes extracellular proteases with high enzyme activity during fermentation (Wang et al., 2022).

* Corresponding authors.
E-mail addresses: sunfangda@neau.edu.cn (F. Sun), kongbh63@hotmail.com (B. Kong).

https://doi.org/10.1016/j.fochx.2024.101204
Received 23 October 2023; Received in revised form 22 December 2023; Accepted 4 February 2024
Available online 8 February 2024

In recent years, commonly used starter cultures of *S. xylosus* and *S. carnosus* have been added to fermented meat products to improve their quality and sensory properties. However, very little work has been conducted on the proteases obtained from these strains isolated from fermented meat products and their effect on the hydrolysis and flavor thereof. Previous, it has been shown that *S. xylosus* produces a high level of proteases in the fermentation system, and an extracellular protease secreted by it has been purified; it is stable at pH 4.0–9.0 and 20–40 °C. In addition, compared with the trypsin and papain, the *S. xylosus* protease exhibited better enzymatic activity on MPs and SPs, especially myosin and actin, and the obtained hydrolysate is non-cytotoxic to HEK-293 cells (Wang et al., 2022). The aim of the present work was to assess the effects of proteases on the hydrolysis, conformation, and flavor properties of MPs and SPs, and the protease secreted by *S. xylosus* come from our previous separation and purification. In addition, a molecular docking simulation study was conducted to explore the interaction mechanisms of the extracellular protease from *S. xylosus* with meat protein. This study provides a basis for the future application of *S. xylosus* protease in meat products.

2. Materials and methods

2.1. Materials

Analytical grade bovine serum albumin (BSA), phosphate, and serine were acquired from Sigma Chemical Co. (St. Louis, MO, USA).

2.2. Extraction and degradation of MPs and SPs

A total of 24 fresh porcine *longissimus* muscles were purchased directly from Beidahuang Meat Corporation (Harbin, Heilongjiang, China), weight per piece was about 25 kg, kept on ice and transported to the laboratory. Every animal (Large white × Duroc crossbred pigs) with a live weight of about 130 kg was held captive and fodder for about 6 months before slaughter. Two *longissimus* muscles for each treatment were used in each replication, and the experiments were independently replicated three times. MPs and SPs were extracted according to the method of Liu et al. (2020). Briefly, minced meat was homogenized with 4 vol (w/v) of buffer A (10 mM $NaH_2PO_4{\cdot}2H_2O$, 10 mM $Na_2HPO_4{\cdot}12H_2O$, 0.1 M NaCl, 2 mM $MgCl_2$, and 1 mM EGTA, pH 7.0), centrifuged at 2, 000 × *g* for 15 min at 4 °C. The supernatant and pellet of the obtained mixture were crude sarcoplasmic proteins and crude myofibrillar proteins, respectively. Among, the supernatant was filtered through four layers of cheesecloth to obtain sarcoplasmic proteins (SPs). The obtained pellet underwent the treatment described above two more times. The myofibril pellet obtained was washed three times with 4 vol of 0.1 mol/L NaCl and centrifuged at 2, 000 × *g* for 15 min at 4 °C. Before the final centrifugation step, the myofibrillar suspension was filtered using four layers of cheesecloth to ensure other impurities were removed, the pH was adjusted to 6 using 0.1 M HCl, and after centrifugation the precipitate collected contained myofibrillar proteins (MPs). The protein concentration was measured by the Biuret method with bovine serum albumin as the standard. The obtained MPs and SPs samples were stored at 4 °C and used within 24 h.

The obtained MPs and SPs were dissolved in 20 mM phosphate buffered at pH 7.0 at a concentration of 10 mg protein/mL. The *S. xylosus* A2 protease come from our previous separation and purification (Wang et al., 2022) and is purified protease, and it (33.3 U/mg) was diluted to 66.6 U/mL using 20 mM phosphate buffered at pH 7.0. A 10 mL of MPs or SPs solution was mixed with 10 mL of protease solution, respectively, and incubated in a rotary shaker (150 rpm) at 37 °C for 0, 5, 10, 20, 30, 60, 90, 120, 150, and 180 min. In addition, the MPs or SPs solution was mixed with the same volume of 20 mM phosphate buffered at pH 7.0, which was control (0 min of hydrolysis).

2.3. Degree of hydrolysis (DH) measurements

The MPs treated with *S. xylosus* protease (protease-treated MPs) and SPs treated with *S. xylosus* protease (protease-treated SPs) solution were heated at 80 °C for 10 min to inactivate of the enzyme. Subsequently, the supernatant was obtained via centrifugation at 4,800 × *g* for 20 min at 4 °C. The DH values were obtained using the method previously published by Li, Wang, Zheng, and Guo (2020). First, 160 mg o-phthaldialdehyde was completely dissolved in 4 mL ethanol, then added to 176 mg dithiothreitol and 150 mL mixture solution containing 7.62 g sodium tetraborate decahydrate and 0.2 g sodium dodecyl sulphate, and finally volumetized to 200 mL by adding deionised water. This mixture was the o-phthaldialdehyde reagent. The protease-treated MPs or SPs was heated in boiling water for 5 min to inactivate the protease, then removed and cooled to 25 °C. A 400 μL MPs or SPs hydrolysate (10 mg/mL) was reacted with 3 mL o-phthaldialdehyde reagent for 5 min. The absorbance value of the solution was detected at 340 nm using a UV-T6 spectrophotometer (Beijing Persee Instruments Co., Ltd., Beijing, China) with serine (0.9516 meqv/L) as a standard.

2.4. Solubility measurements

The suspension of the obtained MPs and SPs samples were diluted to 3.0 mg/mL with phosphate buffered saline (20 Mm, pH 7.0), after which their solubility values were calculated according to the method of Liu et al. (2020).

2.5. Structural characteristics of protease-treated MPs and SPs

2.5.1. Surface hydrophobicity (H_0) analysis

The H_0 values of the protease-treated MPs and SPs solutions were measured using the method reported by Li et al. (2019). The relative fluorescence intensity was plotted against the concentration of the sample.

2.5.2. Fluorescence spectroscopy

Fluorescence spectra of the protease-treated MPs and SPs were obtained by using the method reported by Li et al. (2019).

2.5.3. Fourier transform infrared (FTIR) spectroscopy

FTIR spectra of the protease-treated MPs and SPs were obtained by using the method reported by Niu, Zhang, Xia, Liu, and Kong (2017). The 1700–1600 cm^{-1} regions of the spectral were processed using Peakfit 4.12 software (SPSS Inc., Chicago, IL, USA) to calculate the secondary structures of the proteins (Zhou, Zhao, Cui, & Sun, 2015).

2.6. Micromorphological analysis

The micromorphologies of the protease-treated MPs and SPs were analyzed by using atomic force microscopy (AFM) (Veeco Instruments Inc., Santa Barbara, CA, USA), as described by Liu et al. (2020).

2.7. Emulsifying properties

2.7.1. The emulsifying activity index (EAI) and the emulsion stability index (ESI) measurements

These for the protease-treated MPs and SPs were estimated by using the method of Feng, Ma, Kong, Chen, and Liu (2021).

2.7.2. The microstructure of the emulsions

The morphologies of the emulsions were observed using the method reported by Zhang, Liu, Xia, Sun, and Kong (2021) with slight modifications. The emulsion was prepared via the method described in section 2.7.1. A 30 μL aliquot of emulsion pipetted at 0.5 cm from the bottom of a plastic tube was placed on a microscope slide and covered with a coverslip to visualize the morphology of the emulsions using a 100 × oil

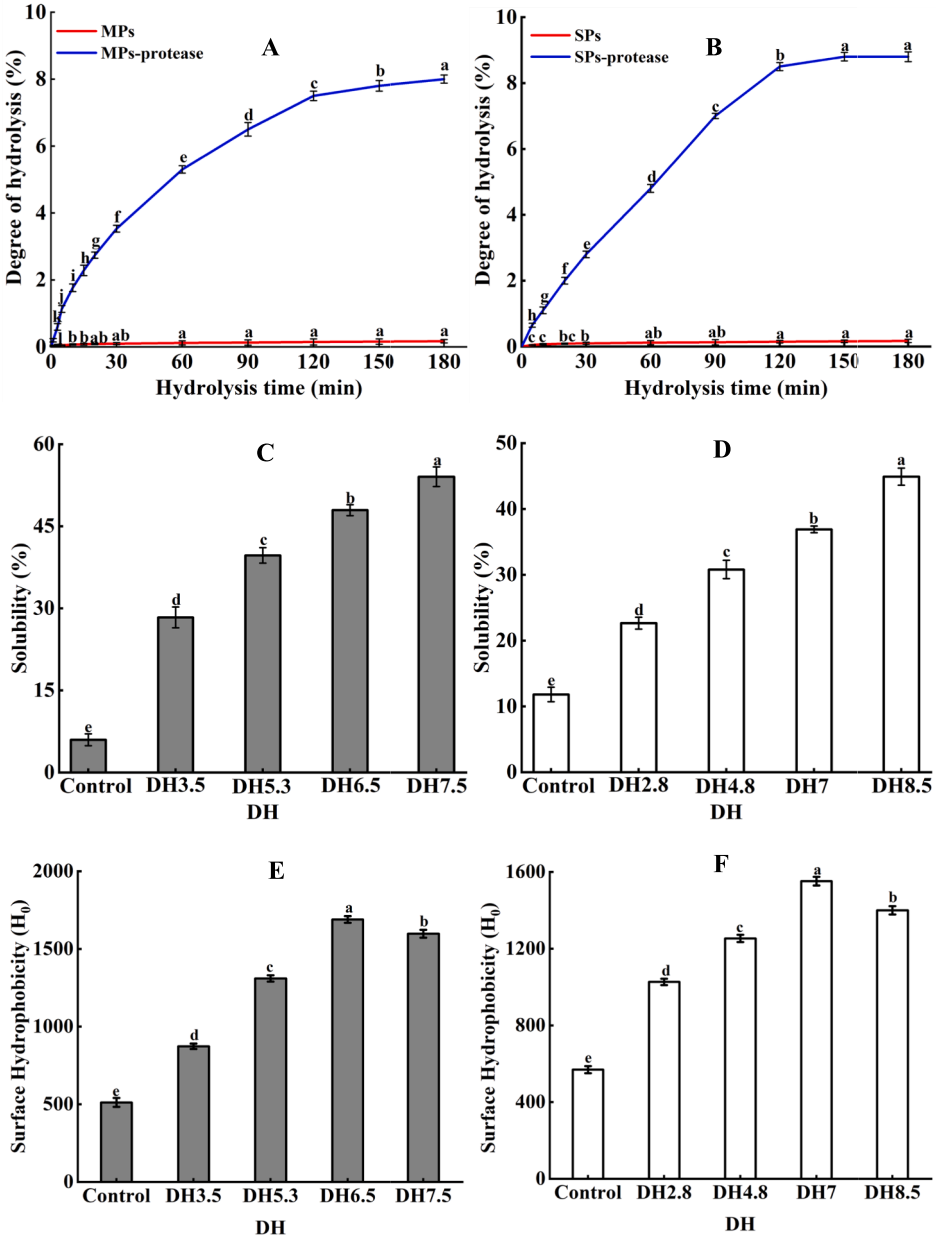

Fig. 1. The degree of hydrolysis (DH) of myofibrillar protein (MPs) (A) and sarcoplasmic protein (SPs) (B) treated with *S. xylosus* protease. The solubility of MPs (C) and SPs (D) treated with *S. xylosus* protease. Structural characteristics of meat proteins MPs (E) and SPs (F) treated with *S. xylosus* protease. Different letters (a-k) in same column indicate significant differences among different treatments ($P < 0.05$).

immersion objective.

2.8. FAAs analysis

The evolution of FAAs in protease-treated MPs and SPs was measured using the method previously published by Chen et al. (2015b).

2.9. Analysis of volatile compounds

Volatile compounds were extracted from the headspace of the meat protein solution according to the method of Chen et al. (2015b). The identified volatile compounds had at least 90 % similarity. Their relative percentages of volatile compounds were calculated via the peak area normalization method.

2.10. Molecular docking studies

The amino acid sequences of *S. xylosus* protease were downloaded from UniProtKB (https://www.UniProt.org/), and its genebank accession numbers were A0A5R9AYG1. In our previous study, the *S. xylosus* protease model was built using an online server (https://swissmodel.expasy.org/), and its ramachandran plot suggests that 95.5 % of the amino acid residues are in reasonable regions, which indicated that the *S. xylosus* protease model is valid (>90 %) (Sun, Wang, Liu, Xia, Chen, & Kong, 2023). The crystal structures of porcine phosphorylase (code: Q5XLD3) and myosin heavy chains (MHCs, code: Q9TV61) were downloaded from the SWISS-MODEL web server (https://swissmodel.expasy.org/). Molecular docking to investigate the *S. xylosus* protease and meat protein interactions was performed using the ZDOCK 3.0.2 software. Ten results were scored by using Vina and analyzed by using PyMOL software.

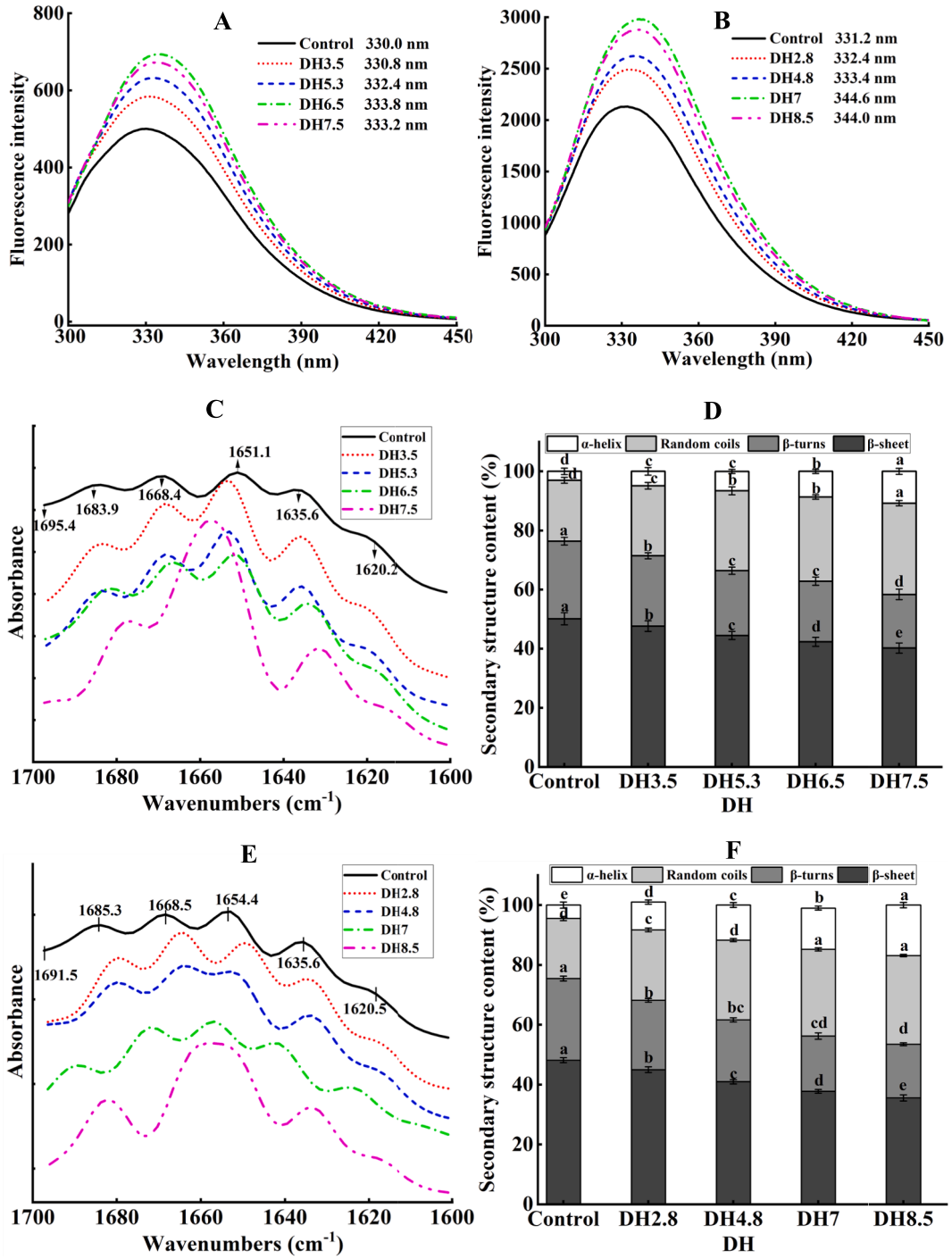

Fig. 2. Intrinsic emission fluorescence spectra of MPs (A) and SPs (B) treated with *S. xylosus* protease. Second derivative FTIR spectra (C) and secondary structure content (D) of MPs treated with *S. xylosus* protease. Second derivative FTIR spectra (E) and secondary structure content (F) of SPs treated with *S. xylosus* protease. Different letters (a-e) in same column indicate significant differences among different treatments ($P < 0.05$).

2.11. Statistical analysis

Three independent batches of the protease-treated MPs and SPs samples were prepared. All measurements were conducted in triplicate. Data are reported as the mean ± standard errors (SE). The data were analyzed via one-way analysis of variance (ANOVA) by using the Statistix 8.1 software package (Analytical Software, St Paul, MN, USA). Statistically significant differences were set as $P < 0.05$.

3. Result and discussion

3.1. Hydrolysis properties

The degree of MPs and SPs hydrolysis over the reaction time of 180 min was investigated using the *S. xylosus* protease, as presented in Fig. 1A and 1B, respectively. With the extension of hydrolysis time, the DH of the protease-treated MPs (Fig. 1A) and SPs (Fig. 1B) increased significantly ($P < 0.05$). For the first 30 min, the DH of the protease-treated MPs and SPs rapidly reached 3.5 % and 2.8 %, respectively,

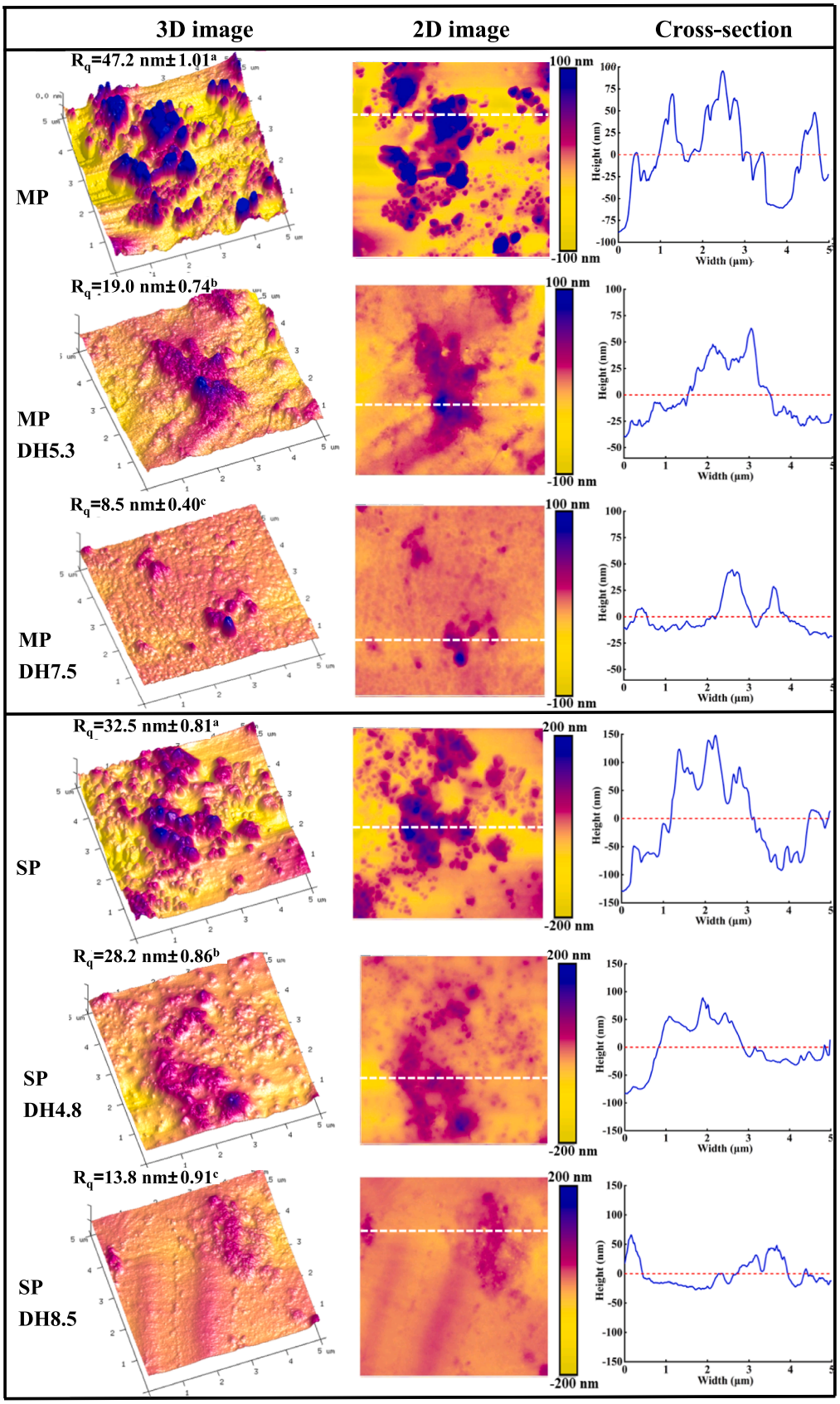

Fig. 3. Representative atomic force microscopy (AFM) images of MPs and SPs suspensions treated with *S. xylosus* protease. The cross-section images represent the section cut with a straight line in the 2D image, which corresponds to the protein surface with the largest roughness. Different letters, (a-c), indicate significant differences in the average roughness value (*Rq*) among different treatments ($P < 0.05$).

and increased to 7.5 % and 8.5 % at 120 min, respectively, while they proceeded slowly after 120 min and plateaued at 8.0 % and 8.8 %, respectively. This might be explained as follows: there are a large number of peptide bonds in the solution at the initial stage of hydrolysis, while a large increase in product concentration may inhibit the progress of the reaction at the later stage of hydrolysis (120–180 min), leading to the accumulation of intermediate complexes to reach a steady-state and tended to be constant, thereby causing a stable degree of hydrolysis (Avramenko, Low, & Nickerson, 2013). In addition, at 60 min, the DH of the protease-treated MPs and SPs were 5.3 % and 4.8 %, respectively, and their DH were 6.5 % and 7 % at 90 min, respectively. This result showed that the protease could hydrolyse MPs and SPs. For the native MPs and SPs, their DH proceeded slowly with the extension of incubation time and was significantly smaller than that of the protease-treated MPs and SPs. This suggests that the activity of meat endogenous protease and microbial is negligible compared to the activity of the *S. xylosus* protease in this study.

At 30, 60, 90, 120 min, the DH of the protease-treated MPs and SPs increased gradually, therefore, these time points were selected for the next test. For the protease-treated MPs, its DH were labelled DH3.5 (30 min), DH5.3 (60 min), DH6.5 (90 min), and DH7.5 (120 min), respectively. Similarly, the DH of protease-treated SPs were labelled DH2.8, DH4.8, DH7, and DH8.5, respectively.

3.2. Protein solubility

A change in solubility is the most notable effect of enzymatic hydrolysis on the protein functional properties. The solubility of protease-treated meat proteins (MPs and SPs) is shown in Fig. 1C and D. The protease-treated MPs and SPs (control) samples showed relatively low solubilities of 5.9 % and 11.8 %, respectively, consistent with the report of Liu et al. (2020), which was mainly related to the low ionic strength in solution. During the whole enzymatic hydrolysis process, the solubilities of protease-treated MPs and SPs were significantly higher than those of the control samples ($P < 0.05$). This can be explained by three effects: i) decreases in disulfide bond content and molecular weight of the protein after the hydrolysis (Zheng et al., 2015); ii) an increased amount of soluble peptides from insoluble aggregates; iii) an increased number of ionizable amino and carboxyl groups exposed on the surface (Ghribi et al., 2015). Similar results have been reported for the limited enzymolysis of rice glutelin and chickpea proteins (Ghribi et al., 2015; Xu et al., 2016).

3.3. Structural characteristics of meat protein

3.3.1. Hydrophobicity changes in MPs and SPs

The hydrophobicity is one of the most important parameters used to evaluate changes in protein conformation and function (Liu et al., 2020). Therefore, the H_0 values were measured to evaluate conformational changes in the protease-treated proteins. The H_0 of the protease-treated MPs (Fig. 1E) and SPs (Fig. 1F) showed a gradual increase with increasing hydrolysis, which suggested that partial hydrolysis induced protein unfolding and exposure of buried Trp/Tyr residues in the MPs and SPs (Avramenko et al., 2013). In contrast, at the highest DH value, the H_0 of the protease-treated MPs and SPs decreased; this could be due to two effects: (1) the hydrophobic areas contributing to the surface hydrophobicity were destroyed with increasing DH; (2) hydrophobic groups exposed to the surrounding water molecules were buried by protein–protein aggregation (Chen, Ettelaie, & Akhtar, 2019). In summary, the protease-treated MPs (DH = 6.5 %) and SP (DH = 7 %) exhibited high H_0 values.

3.3.2. Intrinsic fluorescence spectroscopy

The aromatic amino acids [tryptophan (Trp), tyrosine, and phenylalanine, especially Trp] in proteins are sensitive to the polarity of the environment. Hence, the fluorescence intensity of the protein can reflect the extent of exposure of Trp groups to water, and thus enable the evaluation of changes in the tertiary structure. As shown in Fig. 2A and B, the fluorescence intensities of protease-treated MPs and SPs initially increased with increasing degree of hydrolysis and were higher than those of the control groups; however, they eventually decreased at the highest DH values, which was similar to the result of the surface hydrophobicity. The result suggests that previously buried Trp residues were exposed to water after enzymatic hydrolysis. As the hydrolysis progresses, the polypeptide content increases and the hydrophobic interaction of the polypeptides and peptides becomes stronger; hence, the exposed aromatic groups will be buried again, leading to a new decrease in fluorescence intensity (Xu et al., 2016). Moreover, the maximum value (λ_{max}) of fluorescence emission showed obvious red shift, indicating an increased exposure of the Trp residues to the aqueous solvent (Chen et al., 2019), similar to the results of rice glutelin treated with trypsin (Xu et al., 2016).

3.3.3. FTIR analysis

In general, 1600–1700 cm^{-1} in IR spectra is the most abundant region of proteins secondary structures, and was used to calculate the content of secondary structures in MPs and SPs. The deconvolution spectra of 1600–1700 cm^{-1} in protease-treated MPs shows in Fig. 2C. In 1600–1700 cm^{-1} of untreated MPs, there were six main adsorption bands (centered at 1620.2, 1635.6, 1651.1, 1668.4, 1683.9, and 1695.4 cm^{-1}) (Li et al., 2018) (Fig. 2C). With increasing DH, these absorption bands changed slightly, implying that enzymatic hydrolysis had a strong effect on the secondary structure of MPs (Li et al., 2018). The relative proportions (%) of the MPs secondary structures are shown in Fig. 2D. Compared to the control, the percentages of β-turns (1668.4 cm^{-1}) and β-sheet (1620.2, 1635.6 and 1683.9 cm^{-1}) structures in MPs significantly decreased ($P < 0.05$) with increasing DH, indicating a more flexible protein structure. However, the percentages of α-helical (1651.1 cm^{-1}) and random coil (1695.4 cm^{-1}) structures significantly increased ($P < 0.05$) with increasing DH. As α-helical and random coil structures are more flexible and open, which indicated that hydrolysis caused a more flexible secondary structure in MPs (Xu et al., 2016).

Fig. 2E and F show the deconvolution spectra and secondary structure of treated SPs, respectively. With increasing DH, the percentages of β-turns and β-sheet structures significantly decreased ($P < 0.05$), and the percentages of α-helical and random coil in SPs significantly increased ($P < 0.05$), which demonstrated that treatment with the *S. xylosus* protease can also lead to more flexible secondary structures in SPs.

3.4. Surface morphology analysis

AFM was used to inspect changes in the protein structure (Shi, He, Ding, Wang, & Zhong, 2019). The microstructures of the control and protease-treated meat protein (MPs and SPs) were visualized by AFM, and evaluated by examining 2D and 3D images, as well as cross-sectional images and R_q values (Fig. 3). In the 3D images, the heights of the proteins are marked with different colors, with darker blue colors indicating higher heights. As shown in the 3D and cross-sectional images, the height of MPs and SPs gradually decreased with increasing DH. Furthermore, the R_q value is a highly accurate indicator that can be calculated from the height of all points in the whole region. The R_q values of MPs and SPs showed a significant ($P < 0.05$) decrease with increasing DH. During the overall hydrolysis process, the R_q value of MPs decreased from 47.2 to 8.5 nm, while that of SPs decreased from 32.5 to 13.8 nm; at the same time, the blue color almost disappeared from the images, and evenly distributed red areas gradually appeared and became evenly distributed, which showed that the *S. xylosus* protease could degrade large molecular meat protein (MPs and SPs) to small molecular proteins.

Table 1
Free amino acid contents (mg/100 mL liquid sample) of MPs and SPs (10 mg/mL) treated with S. xylosus protease.

FAA	Degree of hydrolysis – MP						Degree of hydrolysis – SP				
	Control	DH3.5	DH5.3	DH6.5	DH7.5		Control	DH2.8	DH4.8	DH7	DH8.5
Asp	n.d.	0.10 ± 0.01^{d}	0.16 ± 0.01^{c}	0.21 ± 0.01^{b}	0.29 ± 0.01^{a}		n. d.	0.15 ± 0.01^{d}	0.22 ± 0.01^{c}	0.31 ± 0.02^{b}	0.38 ± 0.02^{a}
Glu	0.66 ± 0.02^{e}	0.75 ± 0.03^{d}	0.88 ± 0.04^{c}	0.96 ± 0.03^{b}	1.07 ± 0.05^{a}		0.83 ± 0.02^{e}	0.89 ± 0.04^{d}	0.95 ± 0.03^{c}	1.03 ± 0.03^{b}	1.12 ± 0.04^{a}
Ser	0.24 ± 0.01^{d}	0.26 ± 0.02 ^{cd}	0.29 ± 0.02^{bc}	0.31 ± 0.03^{ab}	0.35 ± 0.03^{a}		0.20 ± 0.01^{d}	0.23 ± 0.01^{d}	0.27 ± 0.02^{c}	0.31 ± 0.02^{b}	0.37 ± 0.02^{a}
Gly	0.73 ± 0.02^{e}	0.85 ± 0.03^{d}	0.92 ± 0.05^{c}	1.03 ± 0.04^{b}	1.11 ± 0.05^{a}		0.55 ± 0.03^{e}	0.61 ± 0.02^{d}	0.70 ± 0.03^{c}	0.78 ± 0.03^{b}	0.86 ± 0.04^{a}
His	0.22 ± 0.01^{e}	0.29 ± 0.02^{d}	0.35 ± 0.03^{c}	0.39 ± 0.02^{b}	0.43 ± 0.03^{a}		0.28 ± 0.02^{e}	0.36 ± 0.04^{d}	0.42 ± 0.03^{c}	0.49 ± 0.03^{b}	0.54 ± 0.04^{a}
Thr	n.d.	0.09 ± 0.01^{c}	0.12 ± 0.01^{b}	0.14 ± 0.02^{b}	0.17 ± 0.01^{a}		1.44 ± 0.07^{e}	1.62 ± 0.08^{d}	1.76 ± 0.07^{c}	1.86 ± 0.07^{b}	1.97 ± 0.09^{a}
Ala	0.74 ± 0.04^{a}	0.75 ± 0.03^{a}	0.75 ± 0.05^{a}	0.76 ± 0.07^{a}	0.77 ± 0.04^{a}		1.33 ± 0.09^{a}	1.35 ± 0.07^{a}	1.38 ± 0.07^{a}	1.41 ± 0.10^{a}	1.45 ± 0.09^{a}
Arg	n.d.	n.d.	n.d.	n.d.	n.d.		n.d.	n.d.	n.d.	n.d.	n.d.
Pro	0.23 ± 0.02^{c}	0.25 ± 0.02^{bc}	0.25 ± 0.01^{bc}	0.26 ± 0.01^{b}	0.29 ± 0.02^{a}		0.32 ± 0.02^{c}	0.35 ± 0.03^{bc}	0.36 ± 0.02^{abc}	0.38 ± 0.02^{ab}	0.41 ± 0.04^{a}
Tyr	0.26 ± 0.02^{e}	0.45 ± 0.03^{d}	0.58 ± 0.04^{c}	0.66 ± 0.04^{b}	0.75 ± 0.05^{a}		0.37 ± 0.02^{e}	0.52 ± 0.03^{d}	0.64 ± 0.04^{c}	0.77 ± 0.06^{b}	0.89 ± 0.06^{a}
Val	n.d.	n.d.	n.d.	n.d.	n.d.		0.63 ± 0.03^{a}	0.64 ± 0.04^{a}	0.64 ± 0.05^{a}	0.65 ± 0.04^{a}	0.66 ± 0.06^{a}
Met	n.d.	n.d.	n.d.	n.d.	n.d.		n.d.	n.d.	n.d.	n.d.	n.d.
Cys	0.71 ± 0.06^{e}	1.03 ± 0.09^{d}	1.38 ± 0.08^{c}	1.79 ± 0.11^{b}	2.02 ± 0.10^{a}		0.73 ± 0.05^{e}	1.11 ± 0.08^{d}	1.32 ± 0.06^{c}	1.63 ± 0.08^{b}	1.85 ± 0.13^{a}
Ile	0.16 ± 0.01^{d}	0.19 ± 0.02 ^{cd}	0.21 ± 0.01^{bc}	0.24 ± 0.02^{ab}	0.27 ± 0.03^{a}		0.13 ± 0.01^{c}	0.17 ± 0.02^{b}	0.19 ± 0.02^{ab}	0.20 ± 0.01^{ab}	0.22 ± 0.02^{a}
Leu	0.40 ± 0.02^{e}	0.52 ± 0.03^{d}	0.63 ± 0.04^{c}	0.74 ± 0.04^{b}	0.83 ± 0.05^{a}		0.54 ± 0.03^{e}	0.67 ± 0.05^{d}	0.76 ± 0.06^{c}	0.87 ± 0.06^{b}	0.98 ± 0.08^{a}
Phe	0.52 ± 0.03^{e}	0.75 ± 0.05^{d}	0.89 ± 0.07^{c}	1.02 ± 0.09^{b}	1.26 ± 0.10^{a}		0.87 ± 0.06^{e}	1.08 ± 0.08^{d}	1.29 ± 0.11^{c}	1.58 ± 0.12^{b}	1.75 ± 0.14^{a}
Lys	0.44 ± 0.02^{c}	0.49 ± 0.03^{bc}	0.53 ± 0.02^{ab}	0.56 ± 0.03^{a}	0.58 ± 0.04^{a}		0.31 ± 0.02^{c}	0.35 ± 0.03^{c}	0.41 ± 0.02^{b}	0.45 ± 0.03^{ab}	0.49 ± 0.04^{a}
Total	5.65 ± 0.14^{e}	7.0 ± 0.17^{d}	8.22 ± 0.13^{c}	9.37 ± 0.17^{b}	10.54 ± 0.19^{a}	2	9.13 ± 0.18^{e}	10.73 ± 0.21^{d}	11.94 ± 0.28^{c}	13.37 ± 0.36^{b}	14.63 ± 0.32^{a}

a–e Means within the same row with different superscript letters differ significantly ($P < 0.05$).
n.d.: not detected. Ser, Serine; Gly, Glycine; Thr, Threonine; Ala, Alanine; Lys, Lysine; Pro, Proline; Asp, Aspartic acid; Glu, Glutamic acid; Arg, Arginine; His, Histidine; Tyr, Tyrosine; Val, Valine; Phe, Phenylalanine; Ile, Isoleucine; Leu, Leucine; Met, Methionine; Cys, Cysteine.

3.5. Emulsifying properties

3.5.1. EAI and ESI analysis

As effective emulsifiers, proteins are commonly used in food emulsions. Their emulsifying properties, including the EAI and ESI parameters, are mainly related to the surface activity of proteins at interfacial layers (Feng et al., 2021). The EAI and ESI values of protease-treated MPs and SPs are shown in Fig. S1A and 1B. The EAI values first increased and then decreased with increasing DH. In fact, the hydrolysis affected the solubility of the proteins, whose surface hydrophobicity was closely related to their emulsifying activity (Jiang et al., 2014). The EAI values of MPs at DH 5.3–6.5 and SPs at DH 4.8–7.0 was significantly higher than those of the corresponding control ($P < 0.05$); this could be because the increase in protein solubility, the decrease in molecular weight, and the exposure of hydrophobic regions promoted the rearrangement and adsorption of protein molecules, thus improving the emulsifying activity (Ghribi et al., 2015). However, the EAI values of the DH7.5 MPs and DH8.5 SPs were significantly lower than those of the control ($P < 0.05$). With increasing DH, an excessive number of protein molecules at the interface could lead to incomplete unfolding and reorientation of the protein, which may result in a reduced emulsifying activity of the treated MPs and SPs (Lam & Nickerson, 2013). Moreover, the trend of the ESI values of treated MPs and SPs was similar to that of the EAI parameter. This can be probably explained by the fact that the interaction between the smaller peptides produced by the hydrolysis generated larger electrostatic repulsion forces at the interface, thus enhancing the viscoelasticity of the film and improving the emulsion stability of the meat protein. However, as the hydrolysis proceeded, the interaction between smaller peptides at the interface decreased; as a result, the viscoelasticity of the formed film was insufficient to prevent the aggregation of neighboring droplets (Avramenko et al., 2013). This result is consistent with the report of Wasswa, Tang, Gu, and Yuan (2007), showing that a moderate hydrolysis can improve the emulsifying properties of meat proteins.

3.5.2. Microstructure of the emulsion

The microstructures of the MPs and SPs emulsions are shown in Fig. S1C and 1D, respectively. The DH5.3 MPs and DH7 SPs showed the smallest oil droplets with the most homogenous distributions, in agreement with the EAI results. In fact, the higher the EAI value of the sample, the smaller the oil droplets and the denser their distribution (Furtado, Mantovani, Consoli, Hubinger, & Cunha, 2017). These changes may be attributed to the greater hydrophobicity of the DH5.3 MPs and DH7 SPs, which led to a stronger interaction between droplets at the protein–oil emulsion interface. According to Evangelho et al. (2017), who studied the functional properties of black bean protein hydrolysates, the formation of small droplets in the emulsion results in improved emulsifying properties, and the low aggregation of the droplets is closely related to a low ionic strength, consistent with the results of this study.

3.6. FAA analysis

The amino acids play a key role in the flavor development of meat products (Chen et al., 2015b). Among, some amino acids have special flavors, while others are taste and flavor precursors (Wen, Li, Han, Chen, & Kong, 2021). We analyzed the FAA compositions and concentrations in MPs and SPs hydrolysates, and the results are shown in Table 1. With

Table 2
Volatile compounds (%) in MPs and SPs (10 mg/mL) treated with S. xylosus protease.

Compound	Degree of hydrolysis – MP					Degree of hydrolysis – SP				
	Control	DH3.5	DH5.3	DH6.5	DH7.5	Control	DH2.8	DH4.8	DH7	DH8.5
Aldehydes (3)										
Nonanal	3.00 ± 0.10^{c}	3.16 ± 0.13^{c}	3.44 ± 0.10^{b}	3.62 ± 0.15^{b}	3.84 ± 0.11^{a}	1.32 ± 0.08^{c}	1.48 ± 0.11^{bc}	1.55 ± 0.14^{abc}	1.68 ± 0.16^{ab}	1.79 ± 0.15^{a}
Pentanal	n. d.	n. d.	n. d.	n. d.	n. d.	0.17 ± 0.02^{a}	n. d.	n. d.	n. d.	n. d.
Hexanal	0.24 ± 0.02^{a}	0.22 ± 0.01^{a}	0.22 ± 0.02^{a}	0.24 ± 0.03^{a}	0.25 ± 0.03^{a}	n. d.	n. d.	n. d.	n. d.	n. d.
Alcohols (7)										
Ethanol	n. d.	0.07 ± 0.01^{d}	0.10 ± 0.01^{c}	0.12 ± 0.02^{b}	0.15 ± 0.01^{a}	0.10 ± 0.01^{e}	0.14 ± 0.01^{d}	0.20 ± 0.02^{c}	0.23 ± 0.03^{b}	0.27 ± 0.03^{a}
(E)-2-Tridecan-1-ol	3.69 ± 0.15^{e}	5.17 ± 0.11^{d}	6.45 ± 0.11^{c}	6.94 ± 0.20^{b}	7.74 ± 0.18^{a}	n. d	n. d.	n. d.	n. d.	n. d.
Hexanol	n. d.	2.28 ± 0.18^{d}	3.05 ± 0.19^{c}	4.16 ± 0.20^{b}	5.11 ± 0.17^{a}	1.54 ± 0.09^{e}	2.36 ± 0.07^{d}	3.54 ± 0.06^{c}	4.24 ± 0.13^{b}	5.06 ± 0.12^{a}
2,3-butanediol	n. d.	0.12 ± 0.02^{d}	0.18 ± 0.01^{c}	0.22 ± 0.01^{b}	0.25 ± 0.02^{a}	n. d	0.07 ± 0.01^{d}	0.13 ± 0.01^{c}	0.17 ± 0.03^{b}	0.21 ± 0.02^{a}
1-Dodecanol	n. d.	n. d.	n. d.	n. d.	n. d.	0.17 ± 0.02^{a}	0.14 ± 0.01^{a}	0.17 ± 0.01^{a}	0.16 ± 0.03^{a}	0.14 ± 0.02^{a}
3-Phenylpropanol	n. d.	0.13 ± 0.01^{d}	0.19 ± 0.03^{c}	0.24 ± 0.02^{b}	0.27 ± 0.02^{a}	n. d.	0.04 ± 0.01^{c}	0.11 ± 0.02^{b}	0.16 ± 0.01^{a}	0.18 ± 0.02^{a}
2-Ethylhexanol	8.26 ± 0.21^{d}	8.57 ± 0.17^{cd}	8.72 ± 0.12^{c}	9.13 ± 0.21^{b}	10.01 ± 0.22^{a}	n. d.	0.17 ± 0.02^{d}	3.44 ± 0.13^{c}	4.21 ± 0.04^{b}	5.51 ± 0.18^{a}
Acids (1)										
Hexanoic acid	n. d.	0.23 ± 0.03^{d}	0.31 ± 0.07^{c}	0.38 ± 0.05^{b}	0.42 ± 0.05^{a}	n. d.	1.79 ± 0.10^{c}	3.11 ± 0.13^{c}	4.51 ± 0.07^{c}	2.97 ± 0.06^{c}
Esters (1)										
Ethyl hexanoate	n. d.	0.52 ± 0.07^{d}	0.78 ± 0.05^{c}	0.95 ± 0.10^{b}	1.15 ± 0.08^{a}	1.33 ± 0.04^{c}	2.27 ± 0.06^{c}	2.82 ± 0.09^{c}	3.46 ± 0.10^{b}	4.34 ± 0.15^{a}
Hydrocarbons (3)										
Tetradecane	n. d.	0.91 ± 0.07^{d}	1.51 ± 0.11^{c}	1.85 ± 0.05^{b}.	2.13 ± 0.13^{a}	n. d.	0.40 ± 0.02^{d}	1.21 ± 0.09^{c}	2.08 ± 0.10^{b}	2.76 ± 0.14^{a}
Octadecane	0.42 ± 0.05^{a}	0.41 ± 0.02^{a}	0.38 ± 0.01^{ab}	0.34 ± 0.01^{bc}	0.32 ± 0.03^{c}	n. d.	n. d.	n. d.	n. d.	n. d.
Heptadecane	n. d.	n. d.	n. d.	n. d.	n. d.	1.01 ± 0.03^{a}	0.92 ± 0.05^{b}	0.88 ± 0.04^{b}	0.82 ± 0.02^{bc}	0.76 ± 0.02^{c}
Other (1)										
2-methoxy-3-Phenol	n. d.	n. d.	n. d.	1.05 ± 0.07^{b}	2.82 ± 0.12^{a}	n. d.	1.81 ± 0.11^{d}	3.68 ± 0.15^{c}	4.29 ± 0.22^{b}	5.98 ± 0.18^{a}

a–e Means within the same row with different superscript letters differ significantly ($P < 0.05$).
n. d.: not detected.

increasing DH, the total concentration of FAAs in MPs and SPs samples increased from 5.65 mg/100 mL to 10.54 mg/100 mL and from 9.13 mg/100 mL to 14.63 mg/100 mL, respectively, which can be attributed to the proteolytic activity of the *S. xylosus* protease. At the DH of 7.5, the main FAA component in MPs was cysteine (0.71 to 2.02 mg/100 mL) followed by phenylalanine (0.52 to 1.26 mg/100 mL), glycine (0.73 to 1.11 mg/100 mL), and glutamic acid (0.66 to 1.07 mg/100 mL). At DH = 8.5, the predominant FAA in SPs was threonine (1.44 to 1.97 mg/100 mL), followed by cysteine (0.73 to 1.85 mg/100 mL), phenylalanine (0.87 to 1.75 mg/100 mL), and glutamic acid (0.83 to 1.12 mg/100 mL). This result indicates that these amino acids may be the main target cleavage sites of the *S. xylosus* protease (Xu, Cao, Zhang, & Yao, 2020). Glycine and glutamic acid, as important FAAs corresponding to "sweet" and "umami" tastes, respectively, could enhance the flavor and taste of products (Chen et al., 2015b). However, increasing the concentration of phenylalanine (whose hydrolysis is associated with a bitter taste) may result in products with a bitter taste. The concentrations of leucine and tyrosine, which are precursors of flavor compounds, also showed significant increases with increasing DH ($P < 0.05$). In fermented meat products, leucine can be converted by aminotransferases to α-keto acids, which are the precursors of malt-flavored aldehydes, fruit-flavored alcohols, and acids (Chen et al., 2015b; Gutsche, Tran, & Vogel, 2012). Increased levels of tyrosine may accelerate the production of toxic tyramine *via* the activity of the decarboxylase enzyme, thereby negatively affecting the flavor of the product (Ardö, 2006). Therefore, only a moderate number of FAAs contributes to the development of flavors in products.

3.7. Analysis of volatile compounds

Flavor compounds from food can be divided into aldehydes, alcohols, esters, ketones, and other categories. Sixteen volatile flavor compounds were identified in treated meat protein (MPs and SPs), including three aldehydes, seven alcohols, one acid, one ester, three hydrocarbons, and another compound (Table 2). Compared with the corresponding control samples, the kinds and percentage of volatile components in treated meat protein (MPs and SPs) showed a significant increase; this indicates that the *S. xylosus* protease promoted the production of aldehydes, acids, alcohols, and other volatile compounds in meat proteins. This could be due to the *S. xylosus* protease accelerating the degradation of meat protein (MPs and SPs) to FAAs, some of which could subsequently generate some volatile compounds (Chen et al., 2015b; Groot & de Bont, 1998).

Aldehydes–As typical products formed by lipid oxidation, aldehydes play a key role in flavor development (Wen et al., 2021). With increasing DH, nonanal (derived from the oxidization of n-9 polyunsaturated fatty acids) was gradually formed in meat protein (MPs and SPs); this could be because a small amount of lipids, retained in the solution during meat protein (MPs and SPs) extraction, was involved in the flavor development (Xiao et al., 2020).

Alcohols–Seven types of alcohols were detected in all protein solutions. Among them, the percentage of ethanol, 3-phenylpropanol, and

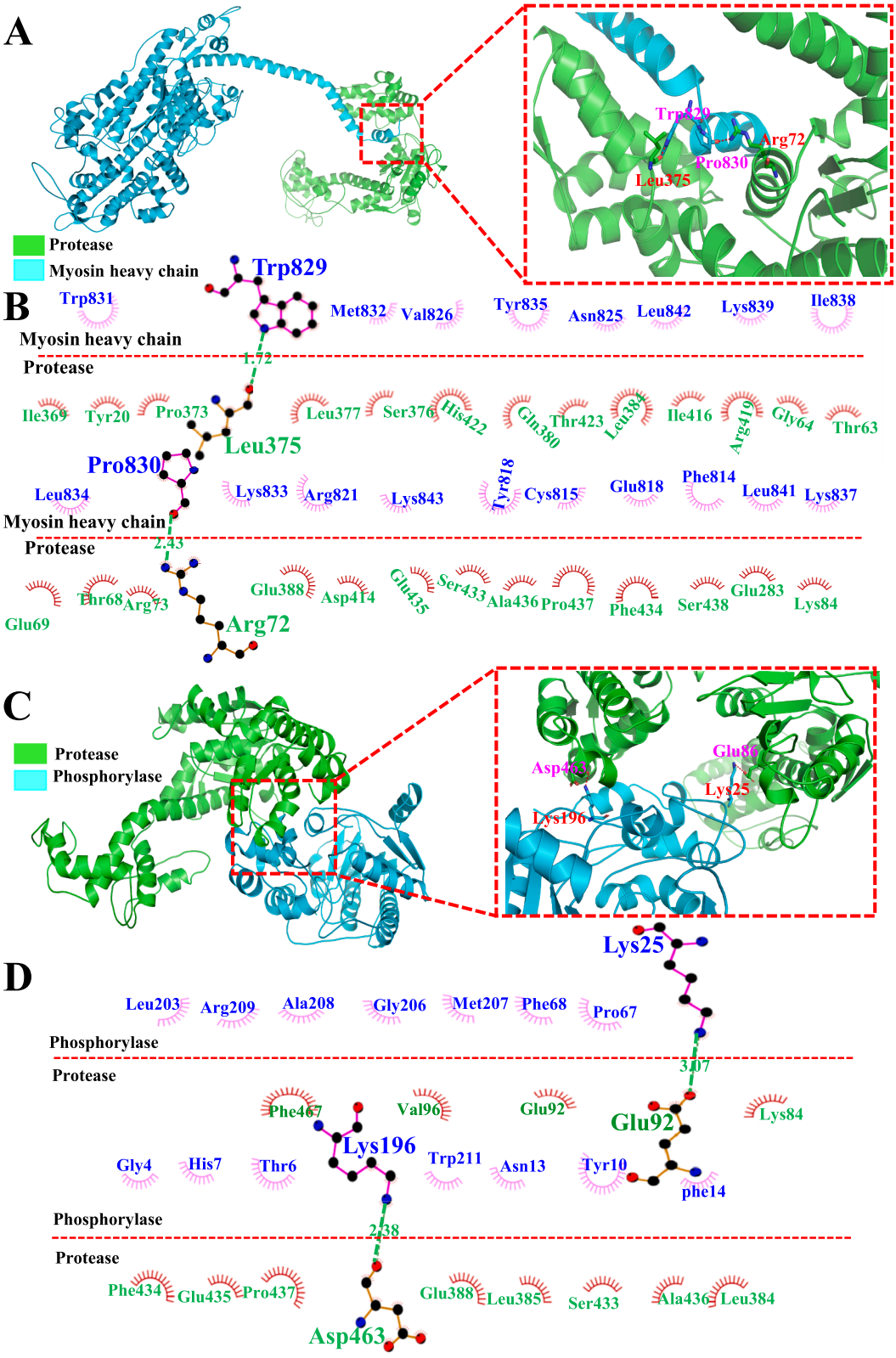

Fig. 4. (A) The best surface docking model of protease (green)- myosin heavy chains (blue). The red and pink letters represent amino acid residues of the protease and myosin heavy chains, respectively. (B) The 2D schematic diagram of the interactions of amino acid residues of the protease and myosin heavy chains. Green letters represent the amino acid residues of the protease; blue letters represent the amino acid residues of the myosin heavy chains; the green dotted line represent hydrogen bond lengths. (C) The best surface docking model of protease (green)-phosphorylase (blue). The red and pink letters represent amino acid residues of the protease and phosphorylase, respectively. (D) The 2D schematic diagram of the interactions of amino acid residues of the protease and phosphorylase. Green letters represent the amino acid residues of the protease; blue letters represent the amino acid residues of the myosin heavy chains; the green dotted line represent hydrogen bond lengths. (For interpretation of the references to color in this figure legend, the reader is referred to the web version of this article.)

2,3-butanediol significantly increased with increasing DH ($P < 0.05$), mainly originating from the amino acid catabolism (Hu et al., 2019; Chen, Kong, Sun, Dong, & Liu, 2015a). This could be due to the *S. xylosus* protease promotes the production of amino acids, and then accelerates the metabolism of amino acids. A higher percentage of hexanol and 2-ethylhexanol was found in the protease-treated MPs and SPs ($P < 0.05$), which may be ascribed to the oxidation of residual lipids (Chen et al., 2015a).

Acids and esters–short-chain fatty acids ($<C_6$) and esters are very important fragrance compounds, and have a significant impact on flavor development, owing to their lower odor detection threshold (Xiao et al., 2020). In this study, only hexanoic acid and ethyl hexanoate were identified in all protein solutions, and their percentages increased during the *S. xylosus* protease treatment. The percentages of hexanoic acid, which originated from the oxidation of hexanol (Hu et al., 2019), was higher in the protease-treated meat protein (MPs and SPs) compared with the native MPs and SPs ($P < 0.05$); this acid was the substrates for ester formation. Ethyl hexanoate derived from the esterification reaction of hexanoic acid with ethanol (Chen et al., 2015a); its percentage was higher in treated than native MPs and SPs ($P < 0.05$), which contributed to the aroma of meat products. Clearly, the *S. xylosus* protease treatment had a positive effect on flavor formation.

3.8. Molecular docking

Previous findings demonstrate that the *S. xylosus* protease has excellent enzymatic activity on the MHCs in MPs and phosphorylase activity on SPs (Wang et al., 2022). Degrading MHCs and phosphorylase, which have important roles in skeletal muscle, can improve the quality and flavor of meat products (Zhou et al., 2020). Therefore, the binding site of *S. xylosus* protease on MHCs and phosphorylase was uncovered via a molecular docking study and the types of interaction and the amino acid residues involved therein were identified. Fig. 4A show the best docking conformations and interaction plots for the protease/MHC complex, respectively. Residues Leu-375 and Arg-72 in the protease are in close contact with residues Try-829 and Pro-830 of an MHC via hydrogen bonds with average bond lengths of 1.72 and 2.43 Å, respectively (Fig. 4B). In addition, other protease residues have extensive hydrophobic interactions with some of the MHC residues.

Fig. 4C show the best docking conformations and interaction plots of the protease/phosphorylase complex, respectively. The active sites of the protease are residues Glu-92 and Asp-463, which form hydrogen bonds with two phosphorylase residues Lys-25 and Lys-196 via hydrogen bond lengths of 3.07 and 2.38 Å, respectively (Fig. 4D). Furthermore, 12 residues of the protease form extensive hydrophobic interactions with 14 amino acid residues of phosphorylase. Finally, MHC and phosphorylase were degraded into peptides or FAAs (Bai et al., 2023; Singh, Vanga, Orsat, & Raghavan, 2018).

4. Conclusions

Our findings demonstrate that the *S. xylosus* protease can significantly enhance the solubility of MPs and SPs ($P < 0.05$). AFM observations reveal that the *S. xylosus* protease can degrade large insoluble aggregates of the native protein to small molecular compounds with uniform distribution and significantly reduced surface roughness ($P < 0.05$). In addition, the protease can degrade MPs and SPs to FAAs, especially glycine, glutamic acid, leucine, and cysteine. The findings from a molecular docking study show that hydrogen bonds and hydrophobic interactions are involved in the formation of an *S. xylosus* protease/meat protein complex. Overall, our results indicate the practicability of using the *S. xylosus* protease in the production of meat products.

CRediT authorship contribution statement

Hui Wang: Writing – original draft, Funding acquisition, Data curation. **Siqi Zhao:** Investigation, Formal analysis. **Xiufang Xia:** Data curation. **Jun Liu:** Software, Resources. **Fangda Sun:** Writing – review & editing, Visualization, Supervision, Conceptualization. **Baohua Kong:** Methodology, Conceptualization.

Declaration of competing interest

The authors declare that they have no known competing financial interests or personal relationships that could have appeared to influence the work reported in this paper.

Data availability

The authors do not have permission to share data.

Acknowledgements

This work has been financed by grants from the Science and Technology Research Project of Henan Province (232102111059) and the Major Science and Technology Project in Henan province (221100110500).

Appendix A. Supplementary data

Supplementary data to this article can be found online at https://doi.org/10.1016/j.fochx.2024.101204.

References

Ardö, Y. (2006). Flavour formation by amino acid catabolism. *Biotechnology Advances, 24*(2), 238–242.
Avramenko, N. A., Low, N. H., & Nickerson, M. T. (2013). The effects of limited enzymatic hydrolysis on the physicochemical and emulsifying properties of a lentil protein isolate. *Food Research International, 51*(1), 162–169.
Bai, G., Pan, Y., Zhang, Y., Li, Y., Wang, J., Wang, Y., Teng, W., Jin, G., Geng, F., & Cao, J. (2023). Research advances of molecular docking and molecular dynamic simulation in recognizing interaction between muscle proteins and exogenous additives. *Food Chemistry, 429*, Article 136836.
Barros, M. R., Menezes, T. M., da Silva, L. P., Pires, D. S., Princival, J. L., Seabra, G., & Neves, J. L. (2019). Furan inhibitory activity against tyrosinase and impact on B16F10 cell toxicity. *International Journal of Biological Macromolecules, 136*, 1034–1041.
Berardo, A., Devreese, B., Maere, H. D., Stavropoulou, D. A., Royen, G. V., Leroy, F., & Smet, S. D. (2017). Actin proteolysis during ripening of dry fermented sausages at different pH values. *Food Chemistry, 221*(15), 1322–1332.
Cachaldora, A., Fonseca, S., Franco, I., & Carballo, J. (2013). Technological and safety characteristics of Staphylococcaceae isolated from Spanish traditional dry-cured sausages. *Food Microbiology, 33*, 61–68.
Chen, L., Ettelaie, R., & Akhtar, M. (2019). Improved enzymatic accessibility of peanut protein isolate pre-treated using thermosonication. *Food Hydrocolloids, 93*, 308–316.
Chen, Q., Kong, B., Sun, Q., Dong, F., & Liu, Q. (2015). Antioxidant potential of a unique LAB culture isolated from Harbin dry sausage: *In vitro* and in a sausage model. *Meat Science, 110*, 180–188.
Chen, Q., Liu, Q., Sun, Q., Kong, B., & Xiong, Y. (2015). Flavour formation from hydrolysis of pork sarcoplasmic protein extract by a unique LAB culture isolated from Harbin dry sausage. *Meat Science, 100*, 110–117.
Chen, X., Xu, X., & Zhou, G. (2016). Potential of high-pressure homogenization to solubilize chicken breast myofibrillar proteins in water. *Innovative Food Science & Emerging Technologies, 33*, 170–179.
Evangelho, J. A., Vanier, N. L., Pinto, V. Z., Berrios, J. J., Dias, A. R., & Zavareze, E. R. (2017). Black bean (Phaseolus vulgaris L.) protein hydrolysates: Physicochemical and functional properties. *Food Chemistry, 214*, 460–467.
Feng, L., Qiao, Y., Zou, Y., Huang, M., Kang, Z., & Zhou, G. (2014). Effect of Flavourzyme on proteolysis, antioxidant capacity and sensory attributes of Chinese sausage. *Meat Science, 98*(1), 34–40.
Feng, Y. Y., Ma, X. L., Kong, B. H., Chen, Q., & Liu, Q. (2021). Ethanol induced changes in structural, morphological, and functional properties of whey proteins isolates: Influence of ethanol concentration. *Food Hydrocolloids, 111*, Article 106379.
Furtado, G. D. F., Mantovani, R. A., Consoli, L., Hubinger, M. D., & Cunha, R. L. D. (2017). Structural and emulsifying properties of sodium caseinate and lactoferrin influenced by ultrasound process. *Food Hydrocolloids, 63*, 178–188.

Ghribi, A. M., Gafsi, I. M., Sila, A., Blecker, C., Danthine, S., Attia, H., Bougatef, A., & Besbes, S. (2015). Effects of enzymatic hydrolysis on conformational and functional properties of chickpea protein isolate. *Food Chemistry, 187*, 322–330.

Gutsche, K. A., Tran, T. B. T., & Vogel, R. F. (2012). Production of volatile compounds by *Lactobacillus sakei* from branched chain α-keto acids. *Food Microbiology, 29*(2), 224–228.

Groot, M. N. N., & de Bont, J. A. M. (1998). Conversion of phenylalanine to benzaldehyde initiated by an aminotransferase in *Lactobacillus plantarum*. *Applied and Environmental Microbiology, 64*, 3009–3013.

Hu, Y., Chen, Q., Wen, R., Wang, Y., Qin, L., & Kong, B. (2019). Quality characteristics and flavor profile of Harbin dry sausages inoculated with lactic acid bacteria and *Staphylococcus xylosus*. *LWT - Food Science and Technology, 114*, Article 108392.

Jiang, L., Wang, J., Li, Y., Wang, Z., Liang, J., Wang, R., Chen, Y., Ma, W., Qi, B., & Zhang, M. (2014). Effects of ultrasound on the structure and physical properties of black bean protein isolates. *Food Research International, 62*, 595–601.

Lam, R. S. H., & Nickerson, M. T. (2013). Food proteins: A review on their emulsifying properties using a structure–function approach. *Food Chemistry, 141*(2), 975–984.

Li, C., Peng, A., He, L., Ma, S., Wu, W., Yang, H., Sun, X., Zeng, Q., Jin, G., Zhang, J., & Ma, M. (2018). Emulsifying properties development of pork myofibrillar and sacroplasmic protein irradiated at different dose: A combined FT-IR spectroscopy and low-field NMR study. *Food Chemistry, 252*(30), 108–114.

Li, F., Wang, B., Liu, Q., Chen, Q., Zhang, H., Xia, X., & Kong, B. (2019). Changes in myofibrillar protein gel quality of porcine longissimus muscle induced by its stuctural modification under different thawing methods. *Meat Science, 147*, 108–115.

Li, Z., Wang, J., Zheng, B., & Guo, Z. (2020). Impact of combined ultrasound-microwave treatment on structural and functional properties of golden threadfin bream (Nemipterus virgatus) myofibrillar proteins and hydrolysates. *Ultrasonics Sonochemistry, 65*, Article 105063.

Liu, H., Zhang, H., Liu, Q., Chen, Q., & Kong, B. (2020). Solubilization and stable dispersion of myofibrillar proteins in water through the destruction and inhibition of the assembly of filaments using high-intensity ultrasound. *Ultrasonics Sonochemistry, 67*, Article 105160.

Niu, H., Zhang, M., Xia, X., Liu, Q., & Kong, B. (2017). Effect of porcine plasma protein hydrolysates on long-term retrogradation of corn starch. *Food Chemistry, 239*, 172–179.

Shi, C., He, Y., Ding, M., Wang, Y., & Zhong, J. (2019). Nanoimaging of food proteins by atomic force microscopy. Part II: Application for food proteins from different sources. *Trends in Food Science & Technology, 87*, 14–25.

Singh, A., Vanga, S. K., Orsat, V., & Raghavan, V. (2018). Application of molecular dynamic simulation to study food proteins: A review. *Critical Reviews in Food Science and Nutrition, 58*, 2779–2789.

Sun, F., Wang, H., Liu, Q., Xia, X., Chen, Q., & Kong, B. (2023). Proteolysis and quality characteristics of Harbin dry sausages caused by the addition of *Staphylococcus xylosus* protease. *Food Chemistry, 404*, Article 134692.

Wang, D., Zhao, L., Su, R., & Jin, Y. (2019). Effects of different starter culture combinations on microbial counts and physico–chemical properties in dry fermented mutton sausages. *Food Sciences and Nutrition, 7*(6), 1957–1968.

Wang, H., Xu, J., Kong, B., Liu, Q., Xia, X., & Sun, F. (2022). Purification and characterization of the protease from *Staphylococcus xylosus* A2 isolated from Harbin dry sausages. *Foods, 11*(8), 1094.

Wasswa, J., Tang, J., Gu, X. H., & Yuan, X. Q. (2007). Influence of the extent of enzymatic hydrolysis on the functional properties of protein hydrolysate from grass carp (Ctenopharyngodon idella) skin. *Food Chemistry, 104*(4), 1698–1704.

Wen, R., Li, X., Han, G., Chen, Q., & Kong, B. (2021). Fungal community succession and volatile compound dynamics in Harbin dry sausage during fermentation. *Food Microbiology, 99*, Article 103764.

Xiao, Y., Liu, Y., Chen, C., Xie, T., & Li, P. (2020). Effect of *Lactobacillus plantarum* and *Staphylococcus xylosus* on flavour development and bacterial communities in Chinese dry fermented sausages. *Food Research International, 135*, Article 109247.

Xu, J. H., Cao, H. J., Zhang, B., & Yao, H. (2020). The mechanistic effect of bromelain and papain on tenderization in jumbo squid (Dosidicus gigas) muscle. *Food Research International, 131*, Article 108991.

Xu, X., Liu, W., Liu, C., Luo, L., Chen, J., Lou, S., McClements, D. J., & Wu, L. (2016). Effect of limited enzymatic hydrolysis on structure and emulsifying properties of rice glutelin. *Food Hydrocolloids, 61*, 251–260.

Zhang, C., Liu, H. T., Xia, X. F., Sun, F. D., & Kong, B. H. (2021). Effect of ultrasound-assisted immersion thawing on emulsifying and gelling properties of chicken myofibrillar protein. *LWT-Food Science and Technology, 142*, Article 111016.

Zhang, S., Zhang, C., Qiao, Y., Xing, L., Kang, D., Khan, I. A., Huang, M., & Zhou, G. (2017). Effect of Flavourzyme on proteolysis, antioxidant activity and sensory qualities of Cantonese bacon. *Food Chemistry, 237*, 779–785.

Zheng, X. Q., Wang, J. T., Liu, X. L., Sun, Y., Zheng, Y. J., Wang, X. J., & Liu, Y. (2015). Effect of hydrolysis time on the physicochemical and functional properties of corn glutelin by Protamex hydrolysis. *Food Chemistry, 172*, 407–415.

Zhou, C. Y., Tang, C. B., Wang, C., Dai, C., Bai, Y., Yu, X. B., Li, C. B., Xu, X. L., Zhou, G., & Cao, J. X. (2020). Insights into the evolution of myosin light chain isoforms and its effect on sensory defects of dry cured ham. *Food Chemistry, 315*, Article 126318.

Zhou, F., Zhao, M., Cui, C., & Sun, W. (2015). Influence of linoleic acid-induced oxidative modifications on physicochemical changes and *in vitro* digestibility of porcine myofibrillar proteins. *LWT-Food Science and Technology, 61*(2), 414–421.